

Slow light loss due to roughness in photonic crystal waveguides: An analytic approach

Weiwei Song, Ryan A. Integlia, and Wei Jiang*

Department of Electrical and Computer Engineering, and Institute for Advanced Materials, Devices and Nanotechnology, Rutgers University, Piscataway, New Jersey 08854, USA

(Received 6 November 2010; published 2 December 2010)

We analytically study roughness-induced scattering loss in a photonic crystal waveguide (PCW). A cross-sectional eigenmode orthogonality relation is derived for a one-dimensional (1D)-periodic system, which allows us to significantly simplify the coupled mode theory in the fixed eigenmode basis. Assisted by this simplification, analytic loss formulas can be obtained with reasonable assumptions despite the complexity of PCW mode fields. We introduce the radiation and backscattering loss factors α_1 and α_2 such that the loss coefficient α can be written as $\alpha = \alpha_1 n_g + \alpha_2 n_g^2$ (n_g is the group index). By finding analytic formulas for α_1 and α_2 , and examining their ratio, we show *why* the backscattering loss *generally* dominates the radiation loss for $n_g > 10$. The interplay between certain mode-field characteristics, such as the spatial phase, and structure roughness is found crucial in the loss-generation process. The loss contribution from each row of holes is analyzed. The theoretical loss results agree well with experiments. Combined with systematic simulations of loss dependences on key structure parameters, the insight gained in this analytic study helps identify promising pathways to reducing the slow light loss. The cross-sectional eigenmode orthogonality may be applicable to other 1D-periodic systems such as electrons in a polymer chain or a nanowire.

DOI: [10.1103/PhysRevB.82.235306](https://doi.org/10.1103/PhysRevB.82.235306)

PACS number(s): 42.70.Qs, 42.25.Fx, 42.79.Gn, 42.82.Et

I. INTRODUCTION

Photonic crystal waveguides (PCWs) can slow down light significantly, which has important applications such as optical switching and modulation¹⁻³ and all optical storage.⁴ However, significant optical loss in the slow light regime stymies further advance in this field. Roughness-induced loss has been previously investigated.⁵⁻¹⁵ The scattering from a single sidewall irregularity was theoretically studied at first.⁶ Random sidewall roughness with spatial correlation was later introduced to account for loss characteristics in real photonic crystal waveguide structures.^{9,10} Although the scaling of slow light loss with respect to the group velocity, v_g , has been examined,^{5,8-16} it has been difficult to reach a conclusive answer. Theory predicted $1/v_g$ scaling for the radiation loss and $1/v_g^2$ scaling for the backscattering loss^{8,9} in the absence of multiple scattering. Experimental studies, however, often fitted the loss data with a simple power law $v_g^{-\nu}$, where ν was found to vary widely.^{10,11,17} To explain these variations, theory should provide a global picture of how the backscattering and radiation losses (and their relative strength) vary with a wide range of structure and roughness parameters commonly found in experiments. More importantly, theory should provide pertinent insight into the loss-generation process and suggest promising pathways to loss reduction.

In this work, we develop a theoretical framework for calculating PCW scattering loss based on the coupled mode theory in the fixed eigenmode basis. Here we will prove an interesting cross-sectional eigenmode orthogonality relation, which allows us to significantly simplify the coupled mode theory in the fixed eigenmode basis. Assisted by this simplification, analytic loss formulas can be obtained with reasonable assumptions despite the complexity of PCW mode fields. We will introduce the radiation and backscattering loss factors α_1 and α_2 , such that the loss coefficient α can be expressed as $\alpha = \alpha_1 n_g + \alpha_2 n_g^2$, where n_g is the group index. By

finding analytic formulas for α_1 and α_2 , and examining their ratio, we show *why* the backscattering loss dominates the radiation loss under fairly general conditions. The analytic study provides further insight into the underpinning physics, such as how the mode-field characteristics (e.g., spatial phase) interact with roughness to produce loss. The dependences of loss on the structure/roughness parameters are simulated to corroborate the analytic results. Unlike numerical studies that are limited to several instances of structures with specific structure/roughness parameters, this analytic study reveals *general* loss characteristics and fresh insight into the loss-generation process, helping identify new pathways to loss reduction.

This paper is organized as follows. In Sec. II, we will present our scattering loss theory. An interesting eigenmode orthogonality relation will be derived and will be utilized to simplify the coupled mode theory in the fixed eigenmode basis. The backscattering and radiation losses will be calculated for the air-bridge type of photonic crystal waveguides, and the loss contribution from each row of holes will be analyzed. In Sec. III, we will present analytic formulas of the backscattering and radiation loss factors and give a general proof of the dominance of the backscattering loss for $n_g > 10$. The interplay between the mode-field characteristics (e.g., spatial phase) and the roughness will be analyzed. In Sec. IV, we will systematically study the loss dependences on the structure and roughness parameters such as the hole diameter, the waveguide width, and the correlation length. Strategies of reducing the roughness-induced loss will be discussed. The theoretical results are found to agree well with experiments. Section V presents our conclusions.

II. SCATTERING LOSS THEORY**A. Coupled mode theory and mode orthogonality in a PCW crosssection**

The coupled mode theory of a photonic crystal waveguide can be written concisely with Dirac notation. This particular

form of coupled mode theory was first developed by Johnson *et al.*¹⁸ for taper transitions in photonic crystals, and was later applied to the disorder-induced scattering problem.¹² The theory can use the fixed eigenmode basis or the instantaneous eigenmode basis. It has the advantage of giving clear dependence of mode coupling on the group velocity through the mode normalization factor. In this theory, the Maxwell's equations are rewritten as¹⁸

$$\hat{A}|\psi\rangle = -i\frac{\partial}{\partial z}\hat{B}|\psi\rangle, \quad (1a)$$

$$\hat{A} = \begin{pmatrix} \omega\varepsilon - \omega^{-1}\nabla_t \times \mu^{-1}\nabla_t \times & 0 \\ 0 & \omega\mu - \omega^{-1}\nabla_t \times \varepsilon^{-1}\nabla_t \times \end{pmatrix}, \quad (1b)$$

$$\hat{B} = \begin{pmatrix} 0 & -\hat{\mathbf{z}} \times \\ \hat{\mathbf{z}} \times & 0 \end{pmatrix}, \quad |\psi\rangle = \begin{bmatrix} \mathbf{E}_t(\mathbf{x}) \\ \mathbf{H}_t(\mathbf{x}) \end{bmatrix}, \quad \mathbf{E}_t \equiv \begin{pmatrix} E_x \\ E_y \end{pmatrix}, \quad (1c)$$

$$\mathbf{H}_t \equiv \begin{pmatrix} H_x \\ H_y \end{pmatrix},$$

where $\varepsilon(\mathbf{X})$ is the dielectric function, μ the permeability. The eigenmodes, $|\psi_\beta\rangle = e^{i\beta z}|\beta\rangle$, satisfy

$$\hat{C}|\beta\rangle \equiv \left(\hat{A} + i\frac{\partial}{\partial z}\hat{B}\right)|\beta\rangle = \beta\hat{B}|\beta\rangle. \quad (2)$$

Here we consider guided and radiation modes with real β . The inner product is defined as

$$\langle\psi|\hat{B}|\psi'\rangle = \hat{\mathbf{z}} \cdot \int \mathbf{E}_t^* \times \mathbf{H}_t' + \mathbf{E}_t' \times \mathbf{H}_t^* dx dy. \quad (3)$$

A rigorous formulation of the coupled mode theory must be established upon a complete set of orthogonal modes.^{18,19} For an ordinary waveguide, whose structure is invariant along z , it is straightforward to show that any two eigenmodes at a given frequency ω must be orthogonal¹⁹

$$\langle\beta|\hat{B}|\beta'\rangle = \eta_\beta\delta_{\beta\beta'}. \quad (4)$$

For a PCW periodic along z , solid-state theory suggests that the eigenstate orthogonality can be obtained only by further integration along z ,

$$\int e^{i(\beta'-\beta)z}\langle\beta|\hat{B}|\beta'\rangle dz = \eta_\beta\delta_{\beta\beta'}. \quad (5)$$

Such an orthogonality relation cannot be directly used in a rigorous PCW coupled mode theory because the modal coupling coefficients also have z dependence and will appear in the above integral. To overcome this problem, a complicated virtual coordinate theory was previously developed.¹⁸

Here we show that Eq. (4) still holds for a PCW in any z section. By partial integration, one can readily show $\langle\beta|\hat{C}|\beta'\rangle = (\langle\beta'|\hat{C}|\beta\rangle)^* + i\frac{\partial}{\partial z}\langle\beta|\hat{B}|\beta'\rangle$. Therefore,

$$(\beta' - \beta)\langle\beta|\hat{B}|\beta'\rangle = i\frac{\partial}{\partial z}\langle\beta|\hat{B}|\beta'\rangle. \quad (6)$$

This is a differential equation of $\langle\beta|\hat{B}|\beta'\rangle_z$ with a solution $\langle\beta|\hat{B}|\beta'\rangle_z = e^{-i(\beta'-\beta)z}\langle\beta|\hat{B}|\beta'\rangle_{z=0}$. However, $\langle\beta|\hat{B}|\beta'\rangle_{z+a} = \langle\beta|\hat{B}|\beta'\rangle_z$ according to Bloch theorem. Therefore, $\langle\beta|\hat{B}|\beta'\rangle = \eta_\beta\delta_{\beta,\beta'-(2n\pi/a)}$, which gives Eq. (4) for β and β' in the first Brillouin zone.

The orthogonality Eq. (4) for a photonic crystal waveguide is an interesting result. According to the Bloch theorem, the eigenstate orthogonality in a generic one-dimensional (1D)-periodic system should be obtained by integrating $\int \psi_b^* \psi_a dz = 0$ along the periodicity direction (z in this case). However, the above proof has shown that if there are multiple eigenstates with different on-axis wave vectors at a given frequency (or photon energy), they must be orthogonal by integrating $\int \psi_b^* \psi_a dx dy$ in any cross section perpendicular to the periodicity axis. Note an equivalent form of this orthogonality was proved in a different theoretical framework based on the Lorentz reciprocity,²⁰ which is limited to electromagnetic wave. The proof given here is generally valid for any scalar or vector wave satisfying Eq. (2). Therefore, the orthogonality relation presented here may be potentially applicable to other 1D-periodic systems, such as electrons in a polymer chain or a nanowire.

The coupled mode theory in the fixed eigenmode basis can now be established easily based on Eq. (4) for a photonic crystal waveguide. With a potential perturbation $\Delta\hat{A}$, the mode equation becomes

$$(\hat{A} + \Delta\hat{A})|\psi\rangle = -i\frac{\partial}{\partial z}\hat{B}|\psi\rangle, \quad (7)$$

where $|\psi\rangle = \sum_n c_n(z)e^{i\beta_n z}|n\rangle$, and $|n\rangle$ are the eigenmodes of the unperturbed system. The coupled mode theory generally requires to use $\langle m|$ to select c_m for a particular mode from Eq. (7). If the conventional orthogonality relation, Eq. (5), is applied, the evaluation of $\int \langle m|\frac{\partial}{\partial z}\hat{B}|\psi\rangle dz$ will be problematic because $c_m(z)$ depends on z . With the orthogonality relation, Eq. (4), however, it is straightforward to show that the coupling coefficients are governed by the following equation:

$$\frac{\partial c_m}{\partial z} = (i/\eta_m) \sum_n e^{i(\beta_n - \beta_m)z} \langle m|\Delta\hat{A}|n\rangle c_n. \quad (8)$$

We should emphasize that although it appears similar to the equation for a conventional waveguide homogenous along z , this simplified Eq. (8) can be *rigorously* established for a PCW only with the help of Eq. (4). This simplification enabled by the cross-sectional orthogonality relation, Eq. (4), is the main improvement for the coupled mode theory used in this work. This simplification allows us to derive analytic loss formulas that can be calculated almost by hand, as we shall see in Sec. III, and provides a clearer physical picture.

B. Separate calculation of backscattering loss and radiation loss

The scattering loss can be introduced through a random potential $\Delta\hat{A}$ due to dielectric perturbation $\Delta\epsilon$ and $\Delta(\epsilon^{-1})$. For a frequency range with a single guided mode $|\beta\rangle$, the perturbed mode is given by

$$|\psi\rangle = c_\beta(z)e^{i\beta z}|\beta\rangle + c_{-\beta}(z)e^{-i\beta z}|-\beta\rangle + \sum_k c_k(z)e^{ik_z z}|k\rangle. \quad (9)$$

where $|k\rangle$ are radiation modes, and $c_m(z)$, $m = \pm\beta, k$ are the coupling amplitudes. With Eq. (4), it is straightforward to solve the coupled mode equations to the first order. For unity input, the output amplitudes are given by

$$c_m = (i/\eta_m) \int \int \int e^{i(\beta-\beta_m)z} (\Delta\hat{A})_{m\beta} dx dy dz,$$

where $(\Delta\hat{A})_{m\beta} \equiv \phi_m^* \Delta\hat{A} \phi_\beta$, $\phi_m = \langle \mathbf{x} | m \rangle$. The loss coefficient is given by the conservation of power flux¹⁹

$$\alpha = (1/L_z) \left[\langle |c_{-\beta}|^2 \rangle + \sum_k \langle |c_k|^2 \rangle |\eta_k / \eta_\beta| \right], \quad (10)$$

where the ensemble average $\langle \cdot \rangle$ over the random roughness has been applied. To show explicit dependence on the group velocity $v_{g,\beta}$ of mode β , we introduce $U_\beta \equiv \frac{1}{4} |\eta_\beta / v_{g,\beta}|$, the time averaged mode energy per unit length along the z axis. For a radiation mode $|k\rangle$, we define $U_k \equiv \frac{1}{4} |\eta_k / v_{g,z,k}|$, where $v_{g,z,k}$ is the z component of $\mathbf{v}_{g,k}$. Then the η_m terms in Eq. (10) can be replaced by U_m and v_g . Assuming that the sidewall roughness of different holes is uncorrelated,⁹ the ensemble averaged α of a PCW is a sum of the ensemble averaged loss contribution from each hole. For roughness-related calculation, it is more convenient to use the polar coordinates (r, θ) in each hole in place of (x, z) . After some calculations, we find

$$\alpha = \alpha_1 n_g + \alpha_2 n_g^2, \quad (11a)$$

$$\alpha_1 = (1/a) \sum_k \sum_{n_x} I(k, \beta, n_x) (c/v_{g,z,k}) |U_k / U_\beta|, \quad (11b)$$

$$\alpha_2 = (1/a) \sum_{n_x} I(-\beta, \beta, n_x), \quad (11c)$$

where n_x and n_z are the indices of holes along x and z , respectively (see Fig. 1). The PCW has a lattice constant a , mean hole radius r_0 , and slab thickness t_{slab} . The integral for the n_x th hole is

$$\begin{aligned} I(m, \beta, n_x) &\equiv (r_0 t_{\text{slab}} / 4 U_m c)^2 \\ &\times \int_{\Omega_{n_x}} e^{i(\beta-\beta_m)r_0(\sin\theta-\sin\theta')} \Delta\hat{A}_{m\beta, n_x}^*(\theta') \Delta\hat{A}_{m\beta, n_x}(\theta) \\ &\times \langle \Delta r(\theta') \Delta r(\theta) \rangle d\theta' d\theta, \end{aligned} \quad (12)$$

where $\Delta\hat{A}_{m\beta, n_x}(\theta) = (1/t_{\text{slab}}) \int \Delta\hat{A}_{m\beta} |_{r=r_0} dy$. A typical autocorrelation function is given by $\langle \Delta r(\theta') \Delta r(\theta) \rangle = \sigma^2 e^{-|\theta-\theta'|r_0/l_c}$, where σ and l_c are the rms roughness and correlation length,

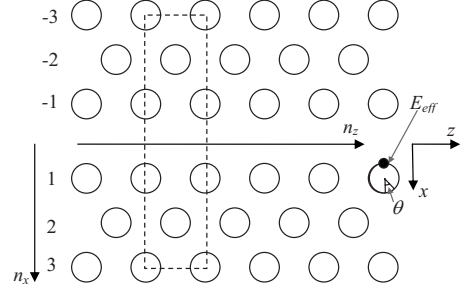


FIG. 1. In-plane view of a line-defect waveguide in a photonic crystal slab.

respectively. Note that the coordinates (r, θ) are centered in each cell Ω_{n_x} .

Now the loss coefficients can be numerically calculated using Eqs. (11) and (12). Instead of directly calculating the loss coefficient α , we will calculate the radiation and backscattering loss factors α_1 and α_2 . Note that α diverges as the frequency approaches the band edge whereas α_1 and α_2 are *slowly varying functions* even near the band edge. Thus the calculation of α_1 and α_2 generally leads to significantly more stable numerical results than directly calculating α .

Here we consider the TE guided modes (i.e., electric field primarily in the xz plane) of a Si air-bridge PCW. The guided modes can be obtained by a preconditioned eigensolver²¹ with a tensorial average of the dielectric constant near interfaces.²² The perturbation potential is evaluated using the continuous components on interfaces.²³

The radiation modes are calculated by considering the PCW supercell delineated in dashed lines in Fig. 1 (the one used in actual calculation is much longer along x) as one period of a two-dimensional grating in the $x-z$ plane. The mode field for a given plane-wave incident upon the PCW top surface can be obtained by any grating diffraction theory.^{24,25} Due to the artificial x periodicity imposed by the grating theory, this treatment is equivalent to calculating the radiation loss for an array of parallel PCWs. For a sufficiently large spacing between waveguides, the radiation losses of adjacent waveguides are independent of each other for weak scattering. Figure 2(a) clearly shows that only the first two rows ($n_x = \pm 1, \pm 2$) contribute significantly to the radiation loss. For each row, data plotted in symbols and lines are obtained by two supercell sizes differing by 50%. Their small differences of α_1 confirm that adjacent waveguides do not affect each other. The backscattering loss shows even stronger dominance by the first row [Fig. 2(b)]. Obviously, this can be attributed to the fact that the scattering matrix elements $\langle -\beta | \Delta\hat{A} | \beta \rangle$ and $\langle k | \Delta\hat{A} | \beta \rangle$ involve $\phi_\beta(x)$, which decays very fast with x .

III. ANALYTIC FORMULAS FOR BACKSCATTERING AND RADIATION LOSSES

Interestingly, the factors α_1 and α_2 roughly have the same order of magnitude in Fig. 2. As a consequence, the backscattering loss ($\alpha_2 n_g^2$) dominates the radiation loss ($\alpha_1 n_g$), which can be seen from their ratio

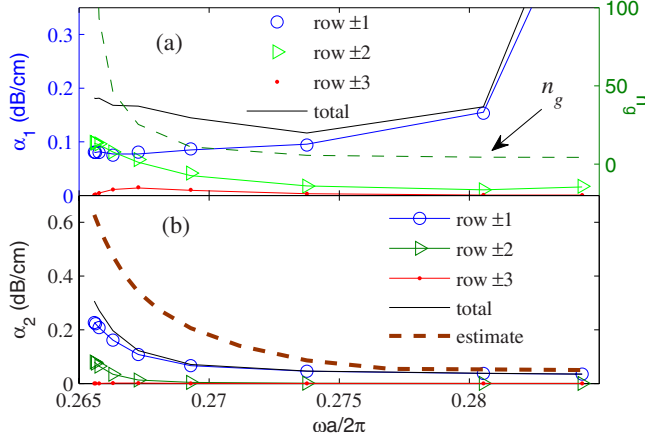


FIG. 2. (Color online) Loss factors as a function of frequency and the contribution from each pair of rows of holes. (a) Radiation loss factor α_1 ; and (b) backscattering factor α_2 and the analytic estimate. PCW parameters: $\alpha=430$ nm, $r_0/a=0.25$, $t_{\text{slab}}=200$ nm, $\sigma=3$ nm, and $l_c=40$ nm.

$$\frac{\alpha_2 n_g^2}{\alpha_1 n_g} \sim n_g \gg 1 \quad (\text{for } n_g > 10).$$

Numerical simulations of a few other PCW structures showed similar dominance.^{9,26} Mathematically, the n_g^2 term surely dominates the n_g term in Eq. (11a) for a sufficiently large n_g . But the n_g threshold for the onset of this dominance depends on α_1 and α_2 and could be too large to be observed (e.g., $n_g > 1000$). To ascertain the universal dominance of backscattering in practically observable n_g ranges and to explore the underpinning mechanism of this dominance, an *analytic* study is needed. Moreover, such a study may offer insight into the interaction between the mode field and roughness.

We have performed analytic calculation of the factor α_2 with some simple reasonable assumptions. As a first step, we assume a guided mode field of the form $E_\beta \sim e^{-\alpha_x x/2} e^{i\beta z}$. After some calculation, we find

$$I(-\beta, \beta, n_x) = (\omega r_0 t_{\text{slab}} / 4 U_{m,c})^2 (\Delta \epsilon_{12})^2 |E_{\text{eff}, n_x}|^4 \sigma^2 I_{\text{ang}},$$

$$I_{\text{ang}} = \int e^{i(2\beta r_0)(\sin \theta - \sin \theta') - \alpha_x r_0 (2 + \cos \theta + \cos \theta')} e^{-|\theta - \theta'| r_0 / l_c} d\theta' d\theta, \quad (13)$$

where $\Delta \epsilon_{12}$ is the dielectric constant difference, E_{eff, n_x} is the effective field at the hole's inner edge ($\theta = \pi$ in Fig. 1). Typically, the correlation length l_c is small. For $e^{-r_0/l_c} \ll 1$, $\alpha_x l_c \ll 1$, and $2\beta l_c \ll 1$, one finds

$$I_{\text{ang}} \approx (4\pi l_c / r_0) \mathcal{I}_0(2\alpha_x r_0), \quad (14)$$

where $\mathcal{I}_0(x) = I_0(x) \exp(-x)$ and I_0 is the modified Bessel function of the first kind. One can show that Eq. (14) still holds for a more general form of the field $E_\beta \sim e^{-\alpha_x x/2} \sum G_U e^{i(\beta+G)z}$ under two scenarios: (1) the mode is dominated by Fourier terms satisfying $G l_c \ll 1$ so that the phase of each e^{iGz} varies little within one correlation length and (2) near the band edge where $\phi_\beta(\mathbf{x}) \approx \phi_{-\beta}(\mathbf{x})$. For the

second scenario, the phases of $\phi_\beta(\mathbf{x})$ and $\phi_{-\beta}^*(\mathbf{x})$ almost exactly cancel each other in $\langle -\beta | \Delta \hat{A} | \beta \rangle$ and become irrelevant. When these conditions are not satisfied, the spatial phase variations tend to reduce I_{ang} below the value given in Eq. (14).

For a guided mode, we can define a modal field amplitude, $\bar{E}_{sp,\beta}$, by $U_\beta = \epsilon_0 \bar{E}_{sp,\beta}^2 w_d t_{\text{slab}} / 2$ and normalize the effective field as $e_{\text{eff},\beta} = E_{\text{eff},\beta} / \bar{E}_{sp,\beta}$. Then combining Eqs. (11c), (13), and (14), we obtain

$$\alpha_2 \approx 2N_{x,\text{back}} \pi (n_1^2 - n_2^2)^2 (k_0^2 \sigma^2 l_c r_0 / a w_d^2) |e_{\text{eff},\beta}|^4 \mathcal{I}_0(2\alpha_x r_0), \quad (15)$$

where $k_0 = 2\pi/\lambda$, $n_1^2 - n_2^2 = \Delta \epsilon_{12} / \epsilon_0$, and $2N_{x,\text{back}}$ is the effective number of rows of holes contributing to backscattering. For numerical estimate, we assume $N_{x,\text{back}} \approx 1$, $w_d = w_0 \equiv \sqrt{3}a$. In addition, $E_{\text{eff},\beta}$ is obtained by averaging $|E_\beta|^2$ at the inner hole edge across the slab thickness. We find that $e_{\text{eff},\beta}$ typically varies around 0.3–0.4 in the slow light regime. The decay constant $\alpha_x \approx 0.77(2\pi/a)$ is obtained by fitting the mode energy against x near the band edge. Note $\mathcal{I}_0(2\alpha_x r_0)$ is a slowly varying function for this parameter range of interest. Figure 2(b) shows that Eq. (15) gives a reasonable estimate of the order of magnitude of α_2 and its trend. There is an overestimate of two to three times because we have neglected the following factors: (a) the vector nature of the field; (b) the high- G Fourier components; and (c) the variation in the field along y .

For the radiation modes, considering two polarizations ($\mu=1,2$) and two propagation directions ($s_z = \pm z$), the sum over k in Eq. (11b) becomes $\sum_k \rightarrow \sum_{\mu, s_z} \frac{L_x L_y}{(2\pi)^2} \int dk_x dk_y$, where L_x and L_y are the transverse dimensions of the normalization volume. Note the final result of α_1 is independent of $L_x L_y$ because $I(k, \beta, n_x) \cdot |U_k| \sim (L_x L_y)^{-1}$ in Eq. (11b). One can then show that

$$\alpha_1 \approx 2N_{x,\text{rad}} (n_1^2 - n_2^2)^2 n_{\text{sub}}^3 (k_0^4 \sigma^2 l_c r_0 t_{\text{slab}} / a w_d) \times |e_{\text{eff},\beta} \bar{e}_{\text{eff},k}|^2 \mathcal{I}_0(\alpha_x r_0), \quad (16)$$

where $\bar{e}_{\text{eff},k}$ is the normalized field amplitude at the hole inner edge averaged over all k states, $n_{\text{sub}} = 1$ is the substrate refractive index, and $2N_{x,\text{rad}}$ is the effective number of rows of holes contributing to radiation loss. Comparing Eq. (15) and Eq. (16), we find

$$\frac{\alpha_1}{\alpha_2} \approx \frac{N_{x,\text{rad}} n_{\text{sub}}^3 k_0^2 w_d t_{\text{slab}}}{\pi N_{x,\text{back}}} \cdot \frac{|\bar{e}_{\text{eff},k}|^2}{|e_{\text{eff},\beta}|^2} \cdot \frac{\mathcal{I}_0(\alpha_x r_0)}{\mathcal{I}_0(2\alpha_x r_0)}. \quad (17)$$

With $N_{x,\text{rad}}, N_{x,\text{back}} = 1 \sim 2$, $w_d = w_0$, $t_{\text{slab}} \sim 220$ nm, $\alpha_x \sim 0.5(2\pi/a)$, and normalized fields $e_{\text{eff},\beta}, \bar{e}_{\text{eff},k} \sim 0.5$, each ratio in Eq. (17) is on the order of unity. This equation therefore predicts that α_1 and α_2 are generally on the same order. Therefore, this analytic study explains why the backscattering generally dominates, $\alpha_2 n_g^2 \gg \alpha_1 n_g$, in the slow light regime $n_g \geq 10$. Note that Eqs. (15) and (16) contain no fast-varying functions, which implies that α_1 and α_2 should be fairly insensitive to most structure parameters for a typical PCW.

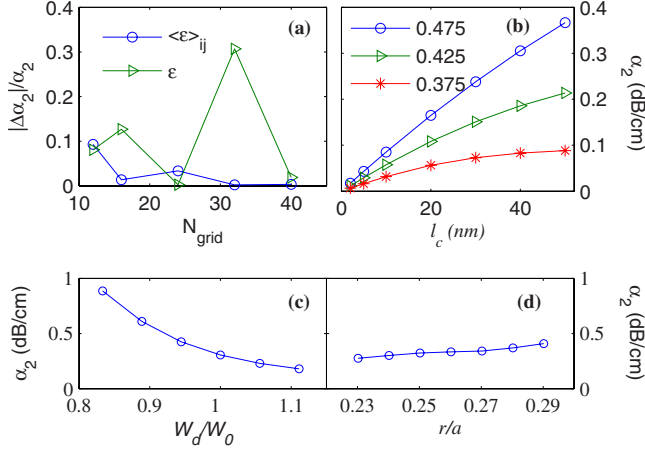


FIG. 3. (Color online) Variation in α_2 with (a) grid size per edge of the unit cell, with tensorial average $\langle \epsilon \rangle_{ij}$ and without (up to 30% oscillation); (b) correlation length l_c , for modes at different $\beta a / 2\pi$; (c) PCW width; and (d) hole radius. PCW parameters: $a=420$ nm, $r_0/a=0.25$, $t_{\text{slab}}=220$ nm, $\sigma=3$ nm, and $l_c=40$ nm.

Note that prior scattering loss formulas still involve the photonic crystal mode field and the Green's function,⁹ which must be obtained through further computation. Our analytic loss formulas, Eqs. (11a), (15), and (16), do not have these terms, and can be evaluated almost by hand. More importantly, the ratio of α_1 and α_2 derived from these formulas, as presented in Eq. (17), gives a *general mathematical* proof of the dominance of the backscattering loss over the radiation loss, along with a predicted dominance threshold $n_g \sim 10$. Prior numerical studies discovered this dominance in a limited number of structures with specific parameters.^{9,26} However, the generality of the dominance and its threshold n_g were not clearly determined in numerical studies.

IV. DISCUSSION

A. Loss dependence on structure and roughness parameters and loss reduction strategy

As the backscattering loss dominates, we focus on the dependences of α_2 on several key roughness/structure parameters. Note that the tensorial average of the dielectric function near interfaces is found to significantly improve the convergence with the spatial grid size, as shown in Fig. 3(a). This allows us to study small structure parameter changes. First, we examine the limitation of the preceding analytic results due to the assumption of small l_c . The dependences of α_2 on l_c for various normalized β values are plotted in Fig. 3(b). For guided modes near the band edge ($\beta a / 2\pi \sim 0.5$), $\alpha_2(l_c)$ is almost perfectly linear. As discussed above, this linearity predicted in Eq. (15) is due to $\phi_\beta(x) \approx \phi_{-\beta}(x)$ near the band edge, which causes phase cancellation in $\langle -\beta | \Delta \hat{A} | \beta \rangle$. Away from the band edge, the phase variation causes the integral I_{ang} to become sublinear at large l_c values [but Eqs. (15) and (16) remain useful as estimates], which is also confirmed in Fig. 3(b). Second, the dependence on the waveguide width is studied in Fig. 3(c). The loss factor α_2 could be reduced by a factor about 5 from $w_d=0.83w_0$ to

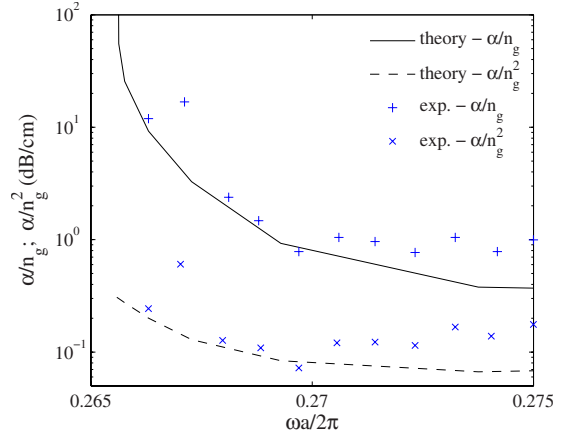


FIG. 4. (Color online) Comparison with experimental results in Ref. 10. The experimental spectrum is shifted to align the band edge with the theory.

$1.1w_0$ near the mode edge. Third, in most experimental works, the air hole diameter and slab thickness usually spread over certain ranges (e.g., $r_0/a:0.23-0.29$ and $t_{\text{slab}}:0.19-0.25$ μm) and the exact values may vary due to uncertainties in fabrication processes. Our simulations show that α_2 varies insignificantly over the typical ranges of a , r_0 , and t_{slab} . The variation of $\alpha_2(\beta a / 2\pi \sim 0.5)$ is plotted against r_0/a in Fig. 3(d).

The analytic and computational studies offer insight into the loss mechanism and point to promising pathways to loss reduction. First, among four essential geometric parameters (r , a , t_{slab} , and w_d), w_d appears to be the *only* one that allows for substantial loss reduction. Second, the spatial phase analysis in the derivation of Eq. (15) suggests that designing guided modes with accentuated high-wave-number Fourier components might help reduce the loss due to *random* roughness. But the eigenfrequency and other *deterministic* characteristics of such a mode also tend to be sensitive to the variations in structure parameters (mean value). Thus, ingenious designs are needed to account for both statistical and deterministic properties. Third, manipulating the polarization, through introducing anisotropic materials, for example, could yield loss much lower than that predicted in Eq. (15), which neglects the polarization. Lastly, Eqs. (15) and (16) and the spatial phase analysis may offer new insight into the mode shaping effect.²⁷

B. Comparison with experiments

In Fig. 4, we compare with experimental results from Ref. 10 using $\sigma=3$ nm and $l_c=40$ nm suggested therein. Evidently, our theory agrees well with experiments for $\tilde{\omega} < 0.273$, including the upswing of the α/n_g^2 ($\approx \alpha_2$) curve near the band edge. This can be partially explained by the fact that the integral of the guided mode intensity $|\mathbf{E}_b(\mathbf{x})|^2$ over the hole surface increases with the group index.²⁷ However, a full explanation must be based on the characteristics of the random potential matrix element $\langle -\beta | \Delta \hat{A} | \beta \rangle$. As discussed above, the phase cancellation in $\langle -\beta | \Delta \hat{A} | \beta \rangle$ causes an increase in I_{ang} and α_2 near the band edge. Due to the interplay

between the spatial phase of the mode and the roughness, this upswing is stronger for larger correlation lengths. Because α_1 and α_2 are not constant *in general*, a simple power law fitting $\alpha \sim n_g^p$ of experimental data would unlikely give consistent ν values, which agrees with the findings of Ref. 27. Note that if the coupling loss^{28,29} is included, the *loss*- n_g relation could even become sublinear (or logarithmic), especially for short waveguides. Above $\tilde{\omega} = \omega a / 2\pi c = 0.273$, the localized band tail states^{21,30} of the second guided mode (band edge $\tilde{\omega} \approx 0.281$) introduce in the experimental spectrum a broad resonance accompanied by a “softened” ν_g at the nominal band edge.³¹ This effect is beyond the scope of this work. Fortunately, this effect can be avoided by designing the second mode above the useful spectral range of the first mode. Below a sufficiently small ν_g , multiple scattering occurs for the first mode, accompanied by undesirably high loss.^{11,26,31–33} The studies presented here could help reduce scattering losses and delay the onset of this regime.

In this work, we have considered loss introduced by guided and radiation modes with real β values. In a nonperturbed photonic crystal structure (including a PCW), modes with complex β values generally arise locally near the end faces and affect the end-face coupling loss³⁴ but not the propagation loss of a truly guided mode. The propagation loss is generally more important for a sufficiently long photonic crystal waveguide. Also within the photonic band gap of a PCW, those modes with complex β values usually do not carry away energy themselves and thus may not introduce propagation loss directly. Some higher order (multiple) scattering processes in a PCW with random perturbations

may involve these modes as an intermediate step. These multiple scattering processes are usually negligible in practically useful (relatively low loss) spectral ranges of photonic crystal waveguides, as discussed in the comparison with experimental data above.

V. CONCLUSION

In summary, analytic formulas, Eqs. (11a), (15), and (16), of the PCW scattering losses can be obtained despite the complexity of the PCW mode fields. With these formulas, the loss of a typical photonic crystal waveguide can be estimated almost by hand. The analytic study reveals that the interplay between the mode characteristics and the structure roughness may hold the key to loss reduction. These results are corroborated by systematic simulations with varying structure parameters. As a byproduct, the cross-sectional eigenmode orthogonality relation for a 1D periodic system may be applicable to other problems, such as electrons in a polymer chain or a nanowire.

ACKNOWLEDGMENTS

We are grateful to David Vanderbilt, Steven G. Johnson, Chee Wei Wong, Philippe Lalanne, Stephen Hughes, Eiichi Kuramochi, Fabian Pease, Leonard C. Feldman, George K. Celler, and George Sigel for helpful discussions. This work is supported by AFOSR MURI under Grant No. FA9550-08-1-0394 (G. Pomrenke).

*Electronic address: wjiangnj@rci.rutgers.edu

- ¹Y. A. Vlasov, M. O’Boyle, H. F. Hamann, and S. J. McNab, *Nature (London)* **438**, 65 (2005).
- ²Y. Q. Jiang, W. Jiang, L. Gu, X. Chen, and R. T. Chen, *Appl. Phys. Lett.* **87**, 221105 (2005).
- ³L. L. Gu, W. Jiang, X. Chen, L. Wang, and R. T. Chen, *Appl. Phys. Lett.* **90**, 071105 (2007).
- ⁴J. T. Mok and B. J. Eggleton, *Nature (London)* **433**, 811 (2005).
- ⁵M. Notomi, K. Yamada, A. Shinya, J. Takahashi, C. Takahashi, and I. Yokohama, *Phys. Rev. Lett.* **87**, 253902 (2001).
- ⁶W. Bogaerts, P. Bienstman, and R. Baets, *Opt. Lett.* **28**, 689 (2003).
- ⁷D. Gerace and L. C. Andreani, *Opt. Lett.* **29**, 1897 (2004).
- ⁸S. G. Johnson, M. L. Povinelli, M. Soljačić, A. Karalis, S. Jacobs, and J. D. Joannopoulos, *Appl. Phys. B: Lasers Opt.* **81**, 283 (2005).
- ⁹S. Hughes, L. Ramunno, J. F. Young, and J. E. Sipe, *Phys. Rev. Lett.* **94**, 033903 (2005).
- ¹⁰E. Kuramochi, M. Notomi, S. Hughes, A. Shinya, T. Watanabe, and L. Ramunno, *Phys. Rev. B* **72**, 161318 (2005).
- ¹¹R. J. P. Engelen, D. Mori, T. Baba, and L. Kuipers, *Phys. Rev. Lett.* **101**, 103901 (2008).
- ¹²M. L. Povinelli, S. G. Johnson, E. Lidorikis, J. D. Joannopoulos, and M. Soljačić, *Appl. Phys. Lett.* **84**, 3639 (2004).
- ¹³B. Wang, S. Mazoyer, J. P. Hugonin, and P. Lalanne, *Phys. Rev. B* **78**, 245108 (2008).
- ¹⁴N. Le Thomas, H. Zhang, J. Jagerska, V. Zabelin, R. Houdre, I. Sagnes, and A. Talneau, *Phys. Rev. B* **80**, 125332 (2009).
- ¹⁵A. Petrov, M. Krause, and M. Eich, *Opt. Express* **17**, 8676 (2009).
- ¹⁶J. F. McMillan, M. Yu, D.-L. Kwong, and C. W. Wong, *Opt. Express* **18**, 15484 (2010).
- ¹⁷L. O’Faolain, T. P. White, D. O’Brien, X. Yuan, M. D. Settle, and T. F. Krauss, *Opt. Express* **15**, 13129 (2007).
- ¹⁸S. G. Johnson, P. Bienstman, M. A. Skorobogatiy, M. Ibanescu, E. Lidorikis, and J. D. Joannopoulos, *Phys. Rev. E* **66**, 066608 (2002).
- ¹⁹D. Marcuse, *Theory of Dielectric Optical Waveguides* (Academic Press, San Diego, 1991).
- ²⁰G. Lecamp, J. P. Hugonin, and P. Lalanne, *Opt. Express* **15**, 11042 (2007).
- ²¹W. Jiang and C. D. Gong, *Phys. Rev. B* **60**, 12015 (1999).
- ²²S. G. Johnson and J. D. Joannopoulos, *Opt. Express* **8**, 173 (2001).
- ²³S. G. Johnson, M. Ibanescu, M. Skorobogatiy, O. Weisberg, J. D. Joannopoulos, and Y. Fink, *Phys. Rev. E* **65**, 066611 (2002).
- ²⁴W. Jiang and R. T. Chen, *J. Opt. Soc. Am. A* **23**, 2192 (2006).
- ²⁵We also used the finite difference time-domain technique but found that it required very long simulation time to obtain the frequency resolutions needed.

- ²⁶S. Mazoyer, J. P. Hugonin, and P. Lalanne, *Phys. Rev. Lett.* **103**, 063903 (2009).
- ²⁷M. Patterson, S. Hughes, S. Schulz, D. M. Beggs, T. P. White, L. O'Faolain, and T. F. Krauss, *Phys. Rev. B* **80**, 195305 (2009).
- ²⁸R. A. Integlia, W. Song, J. Tan, and W. Jiang, *J. Nanosci. Nanotechnol.* **10**, 1596 (2010).
- ²⁹Y. A. Vlasov and S. J. McNab, *Opt. Lett.* **31**, 50 (2006).
- ³⁰S. John, *Phys. Rev. Lett.* **58**, 2486 (1987).
- ³¹M. Patterson, S. Hughes, S. Combrie, N. V.-Quynh Tran, A. De Rossi, R. Gabet, and Y. Jaouen, *Phys. Rev. Lett.* **102**, 253903 (2009).
- ³²S. Mazoyer, P. Lalanne, J. C. Rodier, J. P. Hugonin, M. Spasenović, L. Kuipers, D. M. Beggs, and T. F. Krauss, *Opt. Express* **18**, 14654 (2010).
- ³³J. Topolancik, B. Ilic, and F. Vollmer, *Phys. Rev. Lett.* **99**, 253901 (2007).
- ³⁴W. Jiang, R. T. Chen, and X. J. Lu, *Phys. Rev. B* **71**, 245115 (2005).